2003 Pacific Conference on Earthquake Engineering

# Accuracy of displacement-based seismic evaluation of URM wall stability

M.C. Griffith and G. Magenes

*Department of Civil and Environmental Engineering, The University of Adelaide, Australia*

*Department of Structural Mechanics and ROSE School, The University of Pavia, Italy.*

**ABSTRACT:** A displacement-based method has been proposed recently for assessing the out-of-plane stability of unreinforced masonry (URM) walls. This is an important development given that this particular failure mode is arguably the most commonly observed failure mechanism in earthquakes in regions where URM construction is widespread. The proposed method is simple and recognizes that a masonry wall will not collapse as long as it does not deflect beyond its point of stability. In essence, estimates of displacement demand, obtained from a displacement response spectrum, are compared to the displacement capacity for the wall. The accuracy of this procedure was verified by a limited number of shaking table tests and non-linear dynamic analyses. In the proposed paper, results of a comprehensive, systematic assessment of this simplified procedure are presented. In this assessment, the URM wall parameters of: initial elastic stiffness and period, maximum strength and ultimate (stability) displacement, ground motion frequency content and intensity were all investigated. It is shown that the key parameters for accurate assessment of a wall's seismic demand depend only on a wall's maximum flexural strength and ultimate displacement capacity. It is also shown that these parameters can be predicted with good confidence since they are relatively insensitive to the mechanical properties of the masonry material.

## 1 INTRODUCTION

The seismic resistance of unreinforced brick masonry (URM) construction is widely regarded as poor. Nevertheless, it is a common form of construction in low to moderate earthquake hazard regions such as central and eastern North America, much of Europe, Asia and Australia. Hence, while the earthquake hazard in these regions is modest, so is the seismic resistance of URM construction with the consequence that the seismic risk posed by URM construction is significant. The most commonly observed failure mechanism in URM construction is, arguably, out-of-plane failure of both load-bearing and non-load-bearing walls. It has been recognised for some time that these walls exhibit deformation capacity beyond their "cracking" displacement (e.g. ABK 1984, Giuffré 1989, Priestley, 1985), however quantification of this reserve capacity has been problematic at best. During the late 90s experiments conducted at the University of Adelaide led to the development of a displacement-based procedure for estimating the seismic resistance of URM walls subject to out-of-plane loading (Doherty et al 2002). However, the accuracy of this procedure was based on experiments of two types of walls using four different earthquake ground motions. This paper presents the results of a comprehensive follow-up study at the University of Pavia in Italy (Melis, 2002) that verified the method's accuracy for a wide range of wall geometries, boundary conditions, gravity loading and ground motion characteristics.

## 2 NUMERICAL EVALUATION

Eight 1*m* wide unreinforced brick masonry (URM) walls, restrained against lateral displacement along their bottom and top edges, were analysed using the non-linear finite element analysis package FEAP. The generic normalised static load versus deflection characteristics for all eight walls are shown in Figure 1 where it can be seen that the tri-linear $F-\Delta$ relationship used in the numerical model is contained within the triangular $F-\Delta$ relationship for a static rigid-body analysis of a wall with a horizontal crack at its mid-height and no consideration of deformations (tensile or compressive) in the mortar (refer Figure 2.) The walls' height (*h*) and thickness (*t*), vertical load (*P*), and top edge boundary condition were varied so as to give $F_0/W$ values ranging between 0.1 to 1.0 and $\Delta_U/t$ values between 0.8 and 1.0. The corresponding values for each of the walls are given in Table 1. The set of eight walls considered in this study encompass:

- wall slenderness ratios (*h/t*) ranging between 6 and 30;
- wall heights (*h*) ranging between 3*m* and 5*m*;
- wall thickness (*t*) ranging between 110*mm* and 500*mm*; and
- vertical gravity loads (*P*) ranging between 0 and 0.2*MPa*.

Two boundary conditions were considered along the top edge of the URM walls: the first maintained the vertical load *P* along the wall centreline giving $\Delta_U/t \approx 0.8$; the second placed the vertical load at the edge of the wall face giving $\Delta_U/t = 1$.

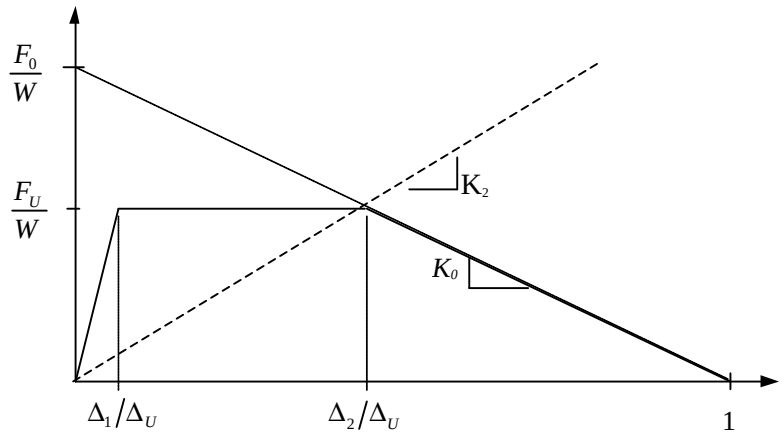


Figure 1. Generic tri-linear force-deformation relationship for URM walls.

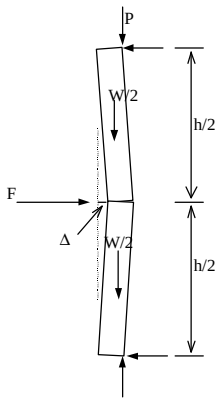


F = $F_0$ when Δ = 0

Δ = $\Delta_U$ at point of instability (i.e. F = 0)

Figure 2. Diagram for static rigid-body analysis of URM wall.

Table 1. Wall properties and $F-\Delta$ characteristics.

| Wall No. | $F_0/W$ | $t$ ($mm$) | $h$ ($m$) | $P$ ($MPa$) | $\Delta_U/t$ |
|---|---|---|---|---|---|
| 1 | 1.01 | 200 | 3 | 0.1 | 0.8 |
| 2a | 0.64 | 300 | 5 | 0.1 | 0.83 |
| 5 | 0.4 | 300 | 3 | 0 | 1.0 |
| 4a | 0.16 | 200 | 5 | 0 | 1.0 |
| 1a | 0.96 | 110 | 3 | 0.2 | 0.78 |
| 6 | 0.67 | 500 | 3 | 0 | 1.0 |
| 3a | 0.47 | 110 | 3.3 | 0.1 | 0.81 |
| 4 | 0.13 | 110 | 3.3 | 0 | 1.0 |

The six earthquake records used to study the influence of different earthquake ground motions are listed in Table 2 (Melis, 2002). Their respective displacement response spectra are given in Figure 3.

Table 2. Earthquake ground motions used in study.

| Earthquake | Description |
|---|---|
| El Centro | Recorded at El Centro during the Imperial Valley, California earthquake, 18th May 1940. Magnitude 6.6, Epicentral Distance 8km. Rock Site. NS component. |
| Taft | Recorded at Kern Country, Taft Lincoln School Tunnel, California, 21st July 1952. S69E component. |
| San Salvador | Recorded at San Salvador, El Salvador, 10th October 1986. Magnitude 5.4, Epicenter 13 67 00N 89 19 00W |
| Artificial | Eurocode 8 compatible earthquake, subsoil class A – rock. |
| Gemona | Recorded at Gemona, Friuli, Italy, 15th September 1976. Magnitude 6.1, NS component |
| Sturno | Recorded at Sturno, Irpinia, Italy, 23rd November1980. Magnitude 6.9, EW component |

The walls were modelled as "equivalent" single-degree-of-freedom (SDOF) systems using the FEAP finite element analysis program. The SDOF system had an equivalent mass equal to the total mass of the wall (although none of the vertical pre-compression load was included as part of the mass) and equivalent viscous damping of 5%. The non-linear force-displacement relationship for the SDOF system was modelled using a tri-linear relationship (as in Figure 1) in terms of $\Delta_1/\Delta_U$ and $\Delta_2/\Delta_U$ and the values in Table 1 for each wall. As noted in Doherty (2000), the dynamic stiffness for the SDOF system is 1.5 times the static stiffness shown in Figure 1 and the support motion must also be multiplied by 1.5 to maintain dynamic similitude between the equivalent SDOF system and the URM wall. With these correlations, the FEAP variable of integration in the equivalent SDOF analysis corresponded directly to the mid-height displacement of the rocking wall system. Values of $\Delta_1/\Delta_U$ and $\Delta_2/\Delta_U$ were varied to study the influence on the walls' dynamic response of the walls' initial stiffness (determined by the position of $\Delta_1/\Delta_U$) and strength (determined by the position of the softening point, $\Delta_2/\Delta_U$).

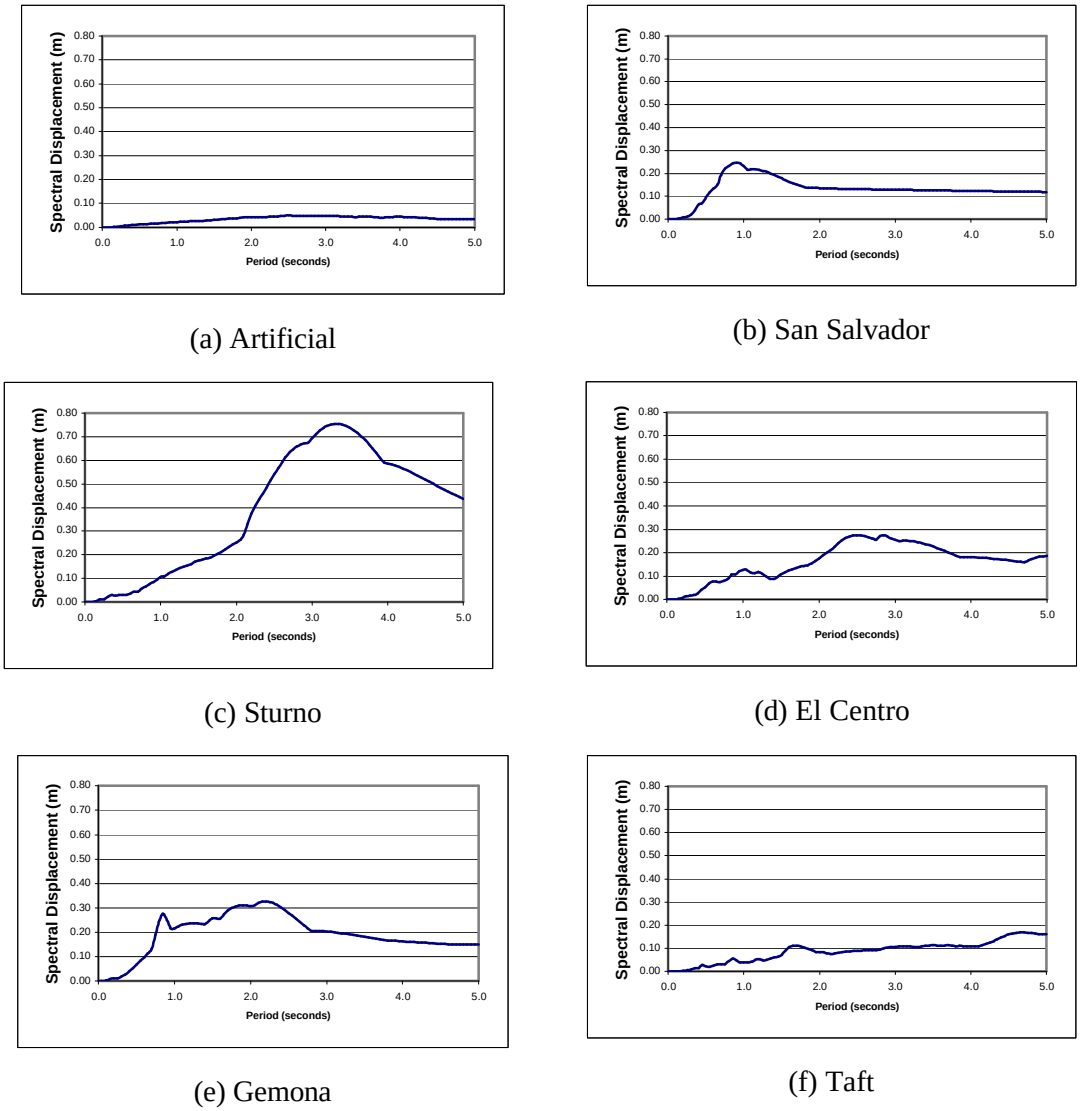


(a) Artificial

(b) San Salvador

(c) Sturno

(d) El Centro

(e) Gemona

(f) Taft

Figure 3. Earthquake records: displacement spectra.

Doherty (2000) conducted an extensive set of non-linear dynamic analyses in order to verify the ability of the tri-linear model to accurately simulate the dynamic response of URM walls subject to earthquake support motion. Melis (2002) analysed several of the walls tested by Doherty (2000) using the FEAP program and confirmed this result.

Having thus confirmed the suitability of the tri-linear model for modelling the out-of-plane response of "simply-supported" URM walls, a more detailed parametric study was conducted to study the effect of the walls' initial stiffness and strength on the post-cracking dynamic response of these walls. An example of the results obtained from these analyses is shown in Figure 4 for Wall 1 where the maximum wall displacement $\Delta_{max}$ (normalised by the theoretical ultimate wall displacement, $\Delta_U$) is plotted versus the "effective" natural period for the wall for a range of ratios for $\Delta_1/\Delta_U$ and $\Delta_2/\Delta_U$. For the two plots on the left-hand side of Figure 4, the data points (from left to right) correspond to the case where $\Delta_2/\Delta_U$ = 0.35 and $\Delta_1/\Delta_U$ = 0.05, 0.075, 0.10, 0.125, 0.15, 0.175 and 0.20, respectively. For the two plots on the right-hand side of Figure 4, the data points (from left to right) correspond to the case where $\Delta_1/\Delta_U$ = 0.10 and $\Delta_2/\Delta_U$ = 0.20, 0.25, 0.30, 0.35, 0.40, 0.45 and 0.50, respectively.

Two methods of period calculation were used for the ordinate of each value of $\Delta_{max}/\Delta_U$ in this figure: $T_1$ and $T_2$. The values of $T_1$ were computed using the stiffness of the initial elastic segment of the tri-linear $F-\Delta$ used in each analysis, i.e. $K_1 = F_U/\Delta_1$ as indicated in Figure 1. The values of $T_2$

were calculated using the secant stiffness going through the point on the tri-linear $F-\Delta$ curve at the point where $\Delta=\Delta_2$, i.e. $K_2=F_U/\Delta_2$ (refer Figure 1). It is of interest to note how sensitive the maximum wall response ($\Delta_{max}/\Delta_U$) is to changes in initial stiffness ($\Delta_1/\Delta_U$) and strength ($\Delta_2/\Delta_U$). From the plots in Figure 4, it appears that the maximum displacement response is moderately sensitive to changes in initial stiffness, although less sensitive for response where $\Delta_{max}/\Delta_U$ <0.5 than it is for large response. Changes in strength seem to have a comparatively small effect on $\Delta_{max}$, regardless of the response magnitude.

The linear elastic displacement response spectra (for 5% damping) are also plotted in Figure 4 to enable comparisons between the displacement spectra and the calculated values. In Figure 4a, it can be seen that for support motion that generates displacement response onto the "plateau" of the $F-\Delta$ curve (i.e. $\Delta_1 \le \Delta_{max} \le \Delta_2$) it appears that good estimates of the wall response can be obtained using the linear elastic response spectra and wall natural period calculated based on the initial stiffness, $T_1$. For displacement response greater than $\Delta_2$ ($\Delta_{max}/\Delta_U$ >0.5, Figure 4b), however, it appears that better estimates of the maximum wall response are given using the elastic spectrum with values of period, $T_2$.

To demonstrate that these trends were consistent for all the walls, $S_d(T)/\Delta_{max}$ is plotted versus $\Delta_{max}/\Delta_U$ for both methods (i.e., using $T_1$ and $T_2$) in Figure 5 for the Artificial (code compatible) earthquake motion and in Figure 6 for the San Salvador (soft soil site) earthquake motion.

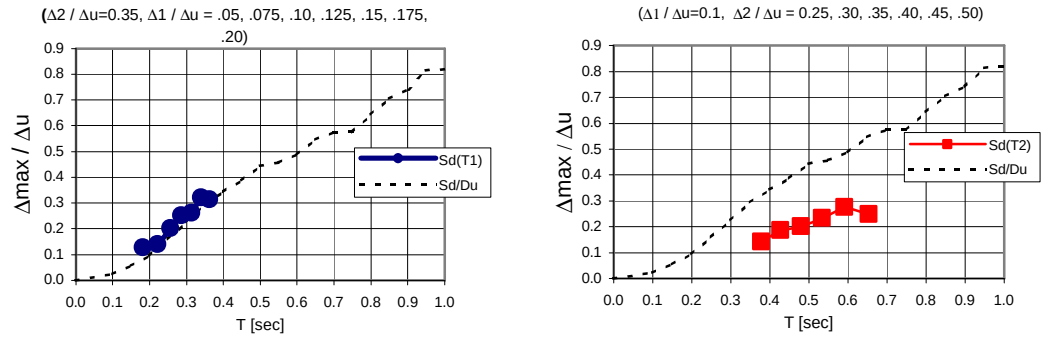


(a) Variation in $\Delta_{max}/\Delta_U$ with changes in $\Delta_1$ and $\Delta_2$ for $\Delta_{max}/\Delta_U < 0.5$.

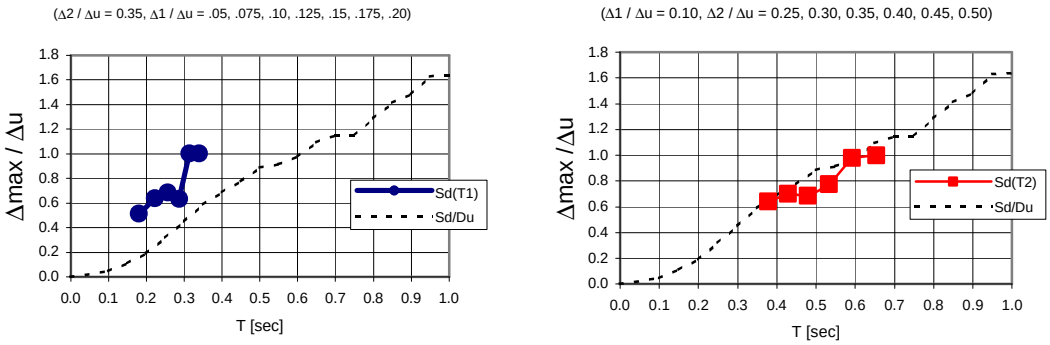


(b) Variation in $\Delta_{max}/\Delta_U$ with changes in $\Delta_1$ and $\Delta_2$ for $\Delta_{max}/\Delta_U > 0.5$.

Figure 4. $\Delta_{max}/\Delta_U$ versus period ($T_1$ or $T_2$) for Wall 1, artificial earthquake.

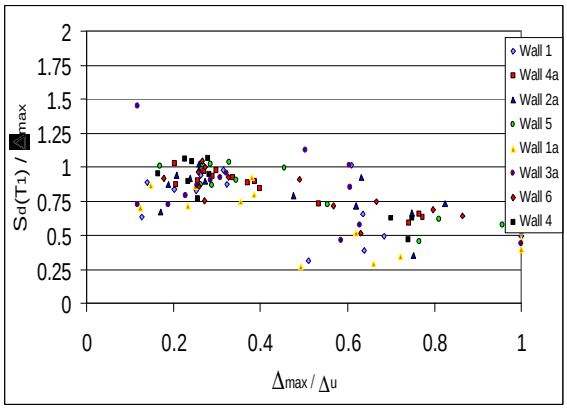


(a) Response predictions using $T_1$ values.

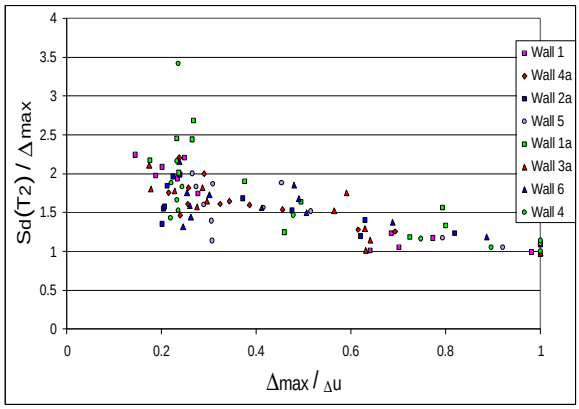


(b) Response predictions using $T_2$ values.

Figure 5. Plots of $S_d / \Delta_{\max}$ values versus $\Delta_{\max} / \Delta_U$ for the Artificial earthquake record.

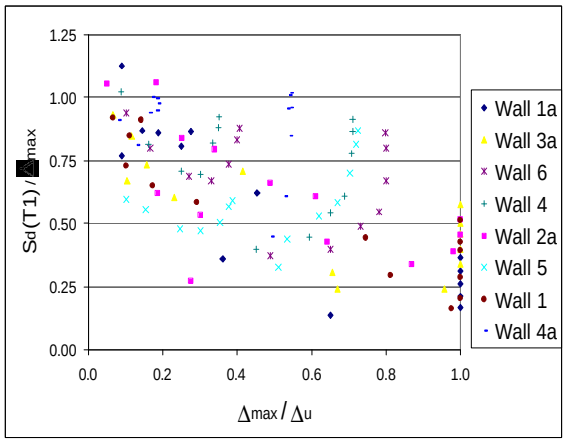


(a) Response spectrum predictions using $T_1$ values for period.

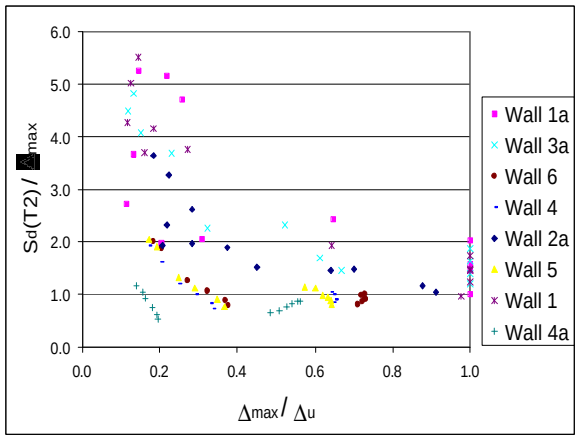


(b) Response spectrum predictions using $T_2$ values for period.

Figure 6. Plots of $S_d / \Delta_{\max}$ values versus $\Delta_{\max} / \Delta_U$ for San Salvador Earthquake.

## 3 DISCUSSION OF RESULTS

Several observations can be made at this point. First, predictions of $\Delta_{\max}$ using $S_d(T_1)$ appear to be mostly within ±25% for maximum displacements less than 50% of $\Delta_U$. However, the spectral estimates are consistently less than the calculated (so-called actual) displacements so while this approach appears to be reasonably accurate, it is also on the "non-conservative" side of the likely "real" maximum values. In other words, it is less likely to predict failure than either the experiments or analysis would suggest. This is especially so in the region of $\Delta_{\max} > 0.5\Delta_U$ where the spectral estimates using $T_1$ are well below the calculated values of $\Delta_{\max}$.

Second, predictions of $\Delta_{\max}$ using $S_d(T_2)$ appear to be generally within ±25% for maximum displacements greater than 50% $\Delta_U$. (A more rigorous statistical evaluation of the accuracy of the predictive method using $T_1$ and $T_2$ is given by Melis (2002)). For this situation, the spectral estimates are generally greater than the calculated displacements so that this approach appears to be both reasonably accurate and also on the "conservative" side of the likely "real" maximum values. It appears that this method, while not giving very good predictions of maximum displacements in the

small amplitude range $(\Delta_{max} < 0.5\Delta_U)$, seems to work reasonably well in the large amplitude $(\Delta_{max} > 0.5\Delta_U)$ displacement region, hence suitable for predicting whether or not a wall will collapse.

Thus, at this stage, it appears that the linear elastic displacement spectra values corresponding to a period calculated using the secant stiffness going through the point on the tri-linear curve where $\Delta = \Delta_2$ will give good predictions of whether or not collapse will occur. In order to see whether this conclusion holds up for a wide range of earthquake types, two walls (Wall 1 and Wall 4a) representing the strongest and weakest in the study, respectively, were reanalysed for all six of the earthquake motions listed in Table 1. The results of these analyses are presented in Figures 7 and 8. It can be seen that the same trends are observed and appear to be quite consistent across all six of the earthquake motions. In fact, the previous observations were observed for the full range of walls and earthquake types considered in the study and are assumed to be generally applicable for all walls with this type of failure mechanism and any earthquake type.

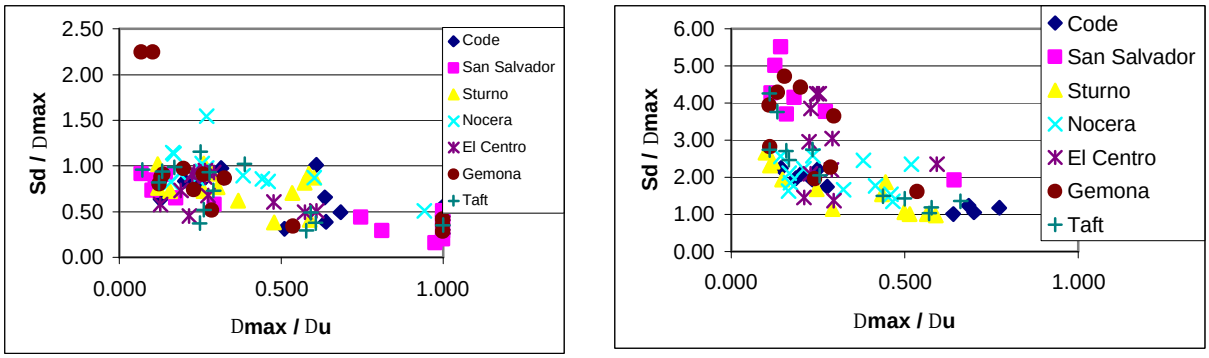


(a) Predictions using $T_1$ values for period. (b) Predictions using $T_2$ values for period.

Figure 7. Variation in $S_d / \Delta_{max}$ values versus $\Delta_{max} / \Delta_U$ for all earthquakes: Wall 1.

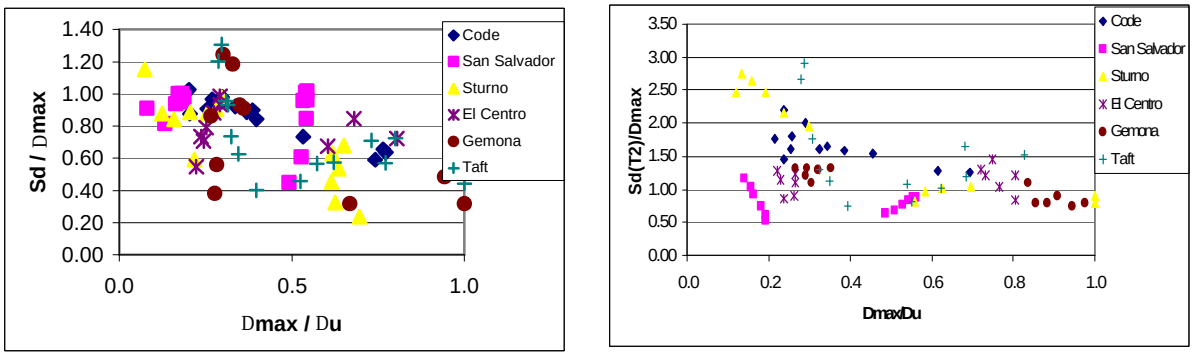


(a) Predictions using $T_1$ values for period. (b) Predictions using $T_2$ values for period.

Figure 8. Variation in $S_d / \Delta_{max}$ values versus $\Delta_{max} / \Delta_U$ for all earthquakes: Wall 4a.

## 4 OBSERVATIONS AND CONCLUDING REMARKS

The triangular envelope for the $F - \Delta$ relationship can be established with a minimum amount of information – wall height, thickness, weight and axial load. The point on the tri-linear $F - \Delta$ curve where $\Delta = \Delta_2$ determines the maximum force plateau, corresponding roughly to the maximum strength of the wall. While Doherty et al (2002) suggest a range of values for $\Delta_2$ (and $\Delta_1$) depending on the condition of the wall, research at the University of Pavia (Picchi 2002) has shown that the maximum wall strength can be calculated using what is essentially the classic "rectangular stress

block" approach (Paulay and Priestley, 1992) and that the strength is relatively insensitive to the wall material properties. With this result, we can see that it is possible to establish a value of $\Delta_2$ for a wall without the need for detailed material property data by using the rigid body analysis triangular envelope and an estimate of the wall strength to intersect the softening slope at the point where $\Delta = \Delta_2$. With this point established, the secant stiffness, $K_2$, can be calculated, giving the corresponding period, $T_2$, with which the collapse assessment can be made using the 5% damped elastic displacement spectra for the earthquake motion being considered.

It has also been observed that spectral displacements calculated using the $T_1$ period values agree reasonably well for response in the range of $\Delta_{max} / \Delta_U < 0.5$. This suggests that for design it may be possible to use an effective secant stiffness approach to check the suitability of walls during the design process. The procedure would still be iterative, requiring checks to ensure that the calculated displacement is in the range of displacement consistent with the secant stiffness value used to obtain the period value used in the design process. Unfortunately, it does not appear at this stage that any single expression for secant stiffness will give sufficiently accurate predictions for the full range of response.

Finally, it still remains to be confirmed whether other failure mechanisms can be modelled in a similar fashion. Work along these lines is currently underway. However, there appears to be no reason, in principle, that it cannot be done if a comparable "rigid body" mechanism exists which has a force-displacement response that can be described with a tri-linear model. It is not quite as clear whether this approach will work when the hysteretic model is not symmetric or when friction (an important component of horizontal bending in 2-way bending mechanisms) is accounted for in the model (i.e., when the non-linear $F - \Delta$ relationship becomes *inelastic* instead of *elastic*).

## 5 **ACKNOWLEDGEMENTS**

The work reported here was undertaken by students Giammichele Melis and Luigino Picchi at the University of Pavia under the supervision of the two authors. Their contributions are gratefully acknowledged. The collaboration between researchers at the University of Adelaide in Australia and the University of Pavia in Italy was made possible by the partial financial support of the INGV-GNDT 2000-2003 framework program.

## REFERENCES:

ABK, 1984. "Methodology for the mitigation of seismic hazards in existing unreinforced masonry buildings: the methodology," *ABK Topical Report 08*, El Segundo, California.

Doherty, K. 2000. An investigation of the weak links in the seismic load path of unreinforced masonry buildings. PhD Thesis, Department of Civil and Environmental Engineering, University of Adelaide.

Doherty, K.T., Griffith, M.C., Lam, N.T.K., and Wilson, J.L., 2002. Displacement-based seismic analysis for out-of-plane bending of unreinforced masonry walls. *Earthquake Engineering and Structural Dynamics*, Vol. 31, No. 4, pp. 833-850.

Giuffré, A., 1989. "Mechanics of historical masonry and strengthening criteria," *Proceedings of the XV Regional Seminar on Earthquake Engineering*, European Association for Earthquake Engineering, Ravello, Italy.

Melis, G. 2002. Displacement-based seismic analysis for out-of-plane bending of unreinforced masonry walls. Masters Dissertation, European School of Advanced Studies in Reduction of Seismic Risk, Rose School, University of Pavia, Italy.

Paulay, T. and Priestley, M.J.N. 1992. "Seismic Design of Reinforced Concrete and Masonry Buildings," John Wiley and Sons, New York.

Picchi, L. 2002. "Risposta sismica per azioni fuori dal piano di pareti murarie – Thesis for the fulfilment of the Laurea degree Civil Engineering, University of Pavia (in Italian).

Priestley, M.J.N. 1985. "Seismic behaviour of unreinforced masonry walls," *Bulletin of the New Zealand National Society for Earthquake Engineering*, Vol.18, No.2, pp. 191-201.